Investigation of the magnetoresistance in EuS/Nb:$SrTiO_3$ junction*

Jia Lu(芦佳)[1], Yu-Lin Gan(甘渝林)[1], Yun-Lin Lei(雷蕴麟)[2], Lei Yan(颜雷)[1,†], and Hong Ding(丁洪)[1,3,4]

[1] *Beijing National Laboratory for Condensed Matter Physics and Institute of Physics, Chinese Academy of Sciences (CAS), Beijing* 100190, *China*

[2] *College of Physics and Materials Science, Tianjin Normal University, Tianjin* 300387, *China*

[3] *Department of Physics, University of Chinese Academy of Sciences, Beijing* 100049, *China*

[4] *CAS Center for Excellence in Topological Quantum Computation, University of Chinese Academy of Sciences, Beijing* 100049, *China*

(Received 21 July 2020; revised manuscript received 10 September 2020; accepted manuscript online 28 September 2020)

EuS is one of typical ferromagnetic semiconductor using as spin filter in spintronic devices, and the doped one could be a good spin injector. Herein, we fabricate a spin-functional tunnel junction by epitaxially growing the ferromagnetic EuS film on Nb-doped $SrTiO_3$. The improvement of Curie temperature up to 35 K is associated with indirect exchange through additional charge carriers at the interface of EuS/Nb:STO junction. Its magnetic field controlled current–voltage curves indicate the large magnetoresistance (MR) effect in EuS barriers as a highly spin-polarized injector. The negative MR is up to 60% in 10-nm EuS/Nb:STO at 4 T and 30 K. The MR is enhanced with increasing thickness of EuS barrier. The large negative MR effect over a wide temperature range makes this junction into a potential candidate for spintronic devices.

Keywords: EuS/Nb:$SrTiO_3$ tunnel junction, spin filter, magnetoresistance

PACS: 75.47.De, 73.43.Qt, 73.50.–h, 75.47.–m **DOI:** 10.1088/1674-1056/abbbf2

1. Introduction

The spintronic technology meets the ever-increasing demand for the faster and lower energy consumption electronic device during the last decade. In the conventional case, the spintronic devices are based on two ferromagnetic electrodes separated by a thin non-magnetic insulating barrier.[1,2] The tunnel current changes depend on relative magnetization orientations in the ferromagnetic electrodes. However, due to the low spin polarized currents of this construction, it is difficult to obtain high-performance devices with full spin polarization degree.[3] An alternative approach is combining with ferromagnetic insulating materials though spin filtering effect. A ferromagnetic insulating barrier as spin filter provides two different tunnel barrier heights.[4,5] When unpolarized electrons across such a tunnel barrier, spin-up and spin-down electrons will cross with different probabilities, thus the transient current changes to be spin-polarized.[6] Since the tunneling probability is exponentially dependent on the barrier height, a spin-filter tunneling junction generates a highly spin-polarized current.[4,5]

The ferromagnetic semiconducting europium chalcogenides EuX (X = O or S) were known as pure Heisenberg ferromagnetic with localized spins since discovered in 1962.[7,8] The physical characteristics such as magnetic, electronic and magneto-optic properties had been researched in the 1960s and 1970s.[9–11] In ferromagnetic phase, divalent Eu in the europium chalcogenide has a half-filled 4f configuration and exhibits a spin polarization close to 100% due to enormous spin splitting of its conduction band. Owing to large magnetic moment and tunable charge carrier concentration of the europium chalcogenides, they have been promising candidates as spin filter in semiconductor spintronic devices.[12–14]

Although the Curie temperature (T_c) of EuO ($\sim$ 69 K) is higher than that of EuS ($\sim$ 16.8 K),[10] it is difficult to grow epitaxial single-crystalline EuO films directly on reactive surfaces like silicon.[15] The fabrication of high-quality EuO tunnel barriers is more complicated than that of EuS, because Eu_2O_3 is more stable than EuO in air atmosphere.[16,17] The continuing attempts to grow EuO/Si heterojunctions are checked by the presence of large amounts of impurity phases at the interface. The impurity phases are not only detrimental to the growth of EuO films, but also prevent spin injection. The low T_c of the stoichiometric insulating EuS limits its application in the spintronic device. However, it has been found that electrons doping and sulfur deficiency can significantly enhance the T_c of EuS.[18–20] Above the T_c of EuS barrier, both spin-up and spin-down electrons experience the same potential barrier, meanwhile, the barrier height becomes spin-dependent due to the spin splitting of the conduction band below T_c.[4,9] Thus, EuS film is suitable for spin filter tunnel barriers and spin injectors allowing spin injection into semiconductors.

Although the EuS thin film has been shown to be effective spin filter,[13,21] however, the investigation of the doped EuS

*Project supported by the Strategic Priority Research Program of the Chinese Academy of Sciences (Grant Nos. XDB28000000 and XDB07000000), the National Key Research and Development Program of China (Grant No. 2016YFA0300600), and the Fund from the Beijing Municipal Science & Technology Commission (Grant No. Z191100007219012).

†Corresponding author. E-mail: lyan@iphy.ac.cn

© 2020 Chinese Physical Society and IOP Publishing Ltd

as spin injector is rarely performed. In present work, the combination of a nonmagnetic metal/ferromagnetic insulator and semiconductor junction was proposed, and EuS was utilized as the spin injector between Nb-doped $SrTiO_3$ semiconductor and Pt metal electrode. EuS is the only magnetic element in this structure without magnetic electrodes, avoiding the decouple of two ferromagnetic electrodes and coherent tunneling. The magnetic field dependence of the tunneling current through the EuS barrier will cause spin-split due to a Zeeman exchange. The spin filter phenomenon of this junction was studied, the tunnel current and MR were also investigated.

2. Experiments

The polycrystal EuS target was prepared from high-purity (99.95%) EuS powder, the powder was enclosed into quartz tubes and sintered at 900 °C, then it was re-grained into powders and pressed into solid disk-like target with 25.4 mm in diameter and 4 mm in thickness. EuS thin films were grown on (100) Nb:$SrTiO_3$ (Nb:STO) single crystal substrates with 0.7 wt% Nb by the pulsed laser deposition (PLD) technique using a 355-nm Nd:YAG solid-state laser. The growth method could be found in elsewhere.[22,23] The base vacuum pressure is 8×10^{-7} Pa. The 10-nm EuS films were grown at 500 °C with 1 J·cm^{-2} laser energy density and 5-Hz repetition. Pt top electrodes about 1×2.5 mm^2 with the thickness about 30 nm were deposited on the top of EuS/Nb:STO with a shadow mask at room temperature, meanwhile, the Pt bottom electrode was deposited on the back side of Nb:STO substrate. The electric contact was Ohmic with a contacting resistance less than 10 Ω at room temperature. The structure of Pt/EuS/Nb:STO/Pt junction is shown as in Fig. 1(a).

The crystal orientation of thin films was measured by x-ray diffraction (XRD) measurement with Cu-$K\alpha$ radiation. Magnetic measurements were performed by a superconducting quantum interference device (SQUID) magnetometer from Quantum Design. The transport measurements were conducted with a magnetic field paralleling the current direction. The dependence of current on voltage (I–V) were measured by four probe method using PPMS. As Nb:STO is an n-type semiconductor, positive bias is defined by the current flowing from top Pt electrode through EuS/Nb:STO to bottom Pt electrode. Measurements were performed in out-of-plane configurations in present work.

3. Results and discussion

Figure 1(b) shows the typical x-ray θ–2θ scans of 10-nm EuS thin film grown on (100) Nb:STO substrate. The (002) and (004) reflections of EuS film is clearly identified. Only preferred orientation along [00l] direction could be found in the XRD pattern which indicates the thin film is well c-axis oriented. In addition, the EDS results confirm the stoichiometric EuS films in all junctions, ruling out the unintended doping.

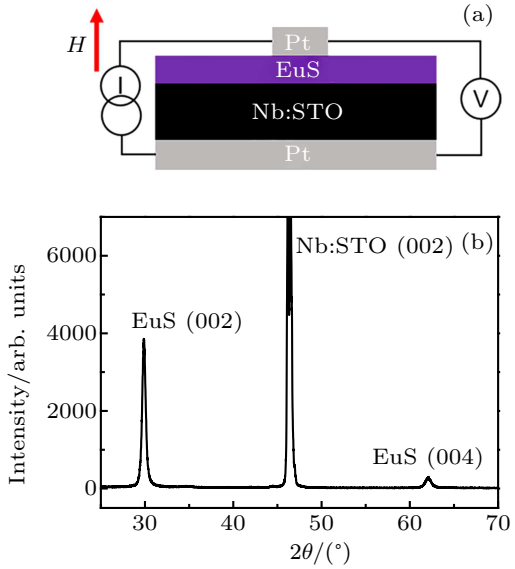


Fig. 1. (a) The cross-section structure of the EuS/Nb:STO junction; (b) the typical XRD pattern of EuS thin film grown on Nb:STO (100) substrate.

As shown in Fig. 2(a), magnetization hysteresis loop of EuS/Nb:STO junction is observed in magnetic measurement with the in-plane magnetic field. The magnetic field sweeps from 0.1 T to −0.1 T and then rise to 0.1 T, the magnetization of the EuS layer is saturated at the coercive field 66.5 Oe (1 Oe = 79.5775 A·m^{-1}), indicating the ferromagnetic property.

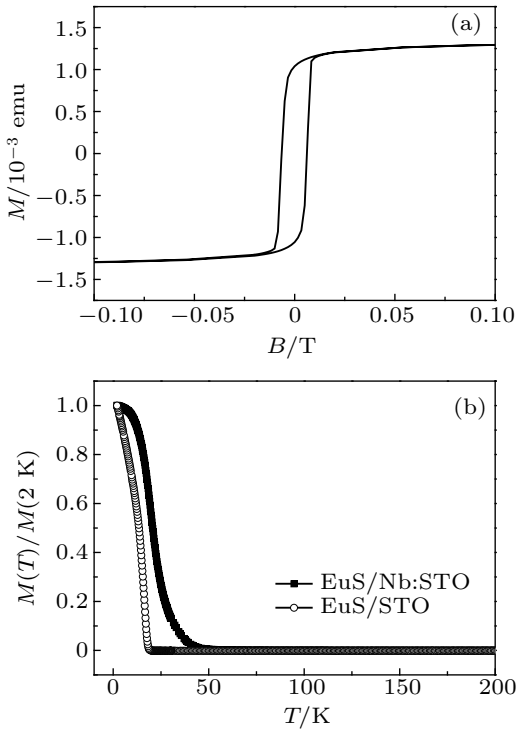


Fig. 2. (a) The in-plane magnetization hysteresis loops of the EuS (10 nm)/Nb:STO junction measured at 2 K; (b) temperature dependences of the normalized magnetization of epitaxial EuS films grown on Nb:STO and STO substrates, respectively, recorded for magnetic field 3-mT applied parallel to the film surface.

The transition temperature of dependent magnetization is detected from the normalized magnetic moment as a function of temperature using the low-field method,[24] as shown in Fig. 2(b). The ferromagnetic transition is observed in M–T curve, where, above 35 K, the EuS film shows a Curie–Weiss-type paramagnetism. The higher T_c indicates the presence of free carrier. The magnetic and transport properties of EuS thin films are strongly depend on the preparation conditions, such as growth temperature, and various substrates.[20,25] Some EuS films grown on undoped STO substrates under the same condition are control samples. The transition temperature of the EuS/STO is about 16.8 K, in agreement with the one observed in the bulk EuS. In addition, the insulting EuS/STO junctions confirms the stoichiometric EuS thin films at our grown conditions. Comparing with the M–T curve of EuS grown on STO, the broadening of the ferromagnetic transition and an enhancement of T_c of EuS/Nb:STO are observed, and this trend is similar to the effects of extrinsic doping in the films. The reason of the enhancement of the T_c maybe associated with indirect exchange through additional charge carriers, which are created at the interface between EuS film and Nb:STO.[20,22,25,26]

The I–V characteristics of the Pt/EuS/Nb:STO/Pt tunneling junctions recorded in zero applied field at various temperatures is shown in Fig. 3(a). Below the T_c ($T < 35$ K), the excess current through the EuS/Nb:STO junction is nonlinear with the applied voltage, which is the typical feature for tunneling of junction.[27] The asymmetry of the I–V curves shows that Nb:STO acts as a metal and EuS as a semiconductor in the junction, the tunnel current with applied positive voltage is smaller than that with applied negative voltage. The carrier injects across the interface barrier, which is consistent with the metallic conductivity of the substrate and the theoretical band structure of EuS. The I–V curves shift to the low bias voltage with the decreasing temperature. This temperature dependence of the I–V characteristics is a manifestation of the effect of a reduction in Schottky barrier height brought about by the strong Zeeman splitting of the conduction band below 35 K.[19] Unlike the conventional junction, the spin-dependent current is always in parallel alignment when external magnetic field applied. The tunnel current is almost symmetry as applying magnetic field at 30 K (as shown in Fig. 3(b)). Compared with the EuS/Al_2O_3 junctions,[5] the junction resistance is quite low because of the additional charge carriers, and show the negative magnetoresistance (MR) effect in low bias voltage. The MR of the junction arise from the Zeeman effect due to the spin dependence of the Schottky barrier, therefore, the Schottky barrier height is influenced by the external applied field.

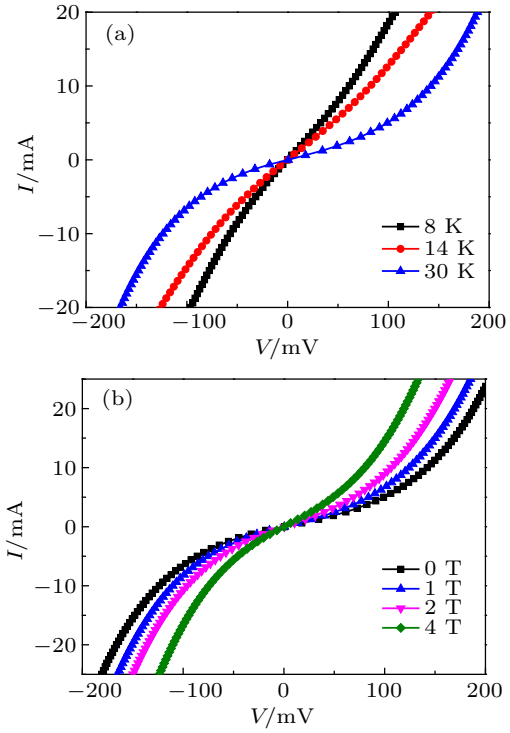


Fig. 3. (a) I–V characteristics of EuS/Nb:STO in zero magnetic field at various temperature; (b) I–V characteristics of EuS/Nb:STO in various magnetic field at 30 K.

The temperature dependence of the junction resistance (R_J) also showed the effect of EuS barrier as spin injector and spin detector. The resistance measurement can show not only the value of T_c, but demonstrate the influence of temperature and magnetic field on the electronic structure of EuS/Nb:STO. As expected for a tunnel junction with a semiconducting barrier, R_J increases as the temperature decreases. When the temperature is below the T_c of EuS, lowering of the tunnel barrier height for spin-up electrons due to exchange splitting of the conduction band results in a significant decrease of R_J with decreasing temperature. Figure 4(a) presents the temperature dependence of the resistance of the heterojunction in different external fields. The resistance of this junction exhibits semiconducting behavior as temperature decreasing firstly and change to metal-like below 36 K in the zero external magnetic field, which is constant with the $M(T)$ curve in Fig. 2(b), indicates the ferromagnetic transition at 36 K. The peak in resistance near T_c is well known from the studies on europium chalcogenides,[28] the maximum is caused by charge carriers spin scattering on the critical magnetic fluctuations, the qualitatively model is given by de Gennes and Friedel,[29] this scattering decreases the mobility of the electrons which participate in band conduction. As the external magnetic field increasing, the transition shifts toward higher temperature as well as the resistance decrease. Namely, the resistance is influenced by the magnetic field, the magnetic field moves the maximum of $R(T)$ towards higher temperatures, reduces the magnitude of the resistivity peak, and broadens the peak with magnetic field raising from 0.1 T to 4 T. The large decrease in R_J caused by

the application of magnetic field near T_c maybe due largely to a field-induced increase in the mobility, which is confirmed in Fig. 3(b). Additionally, R_J decreases as temperature increases consistent with tunnel transport at temperature above T_c.

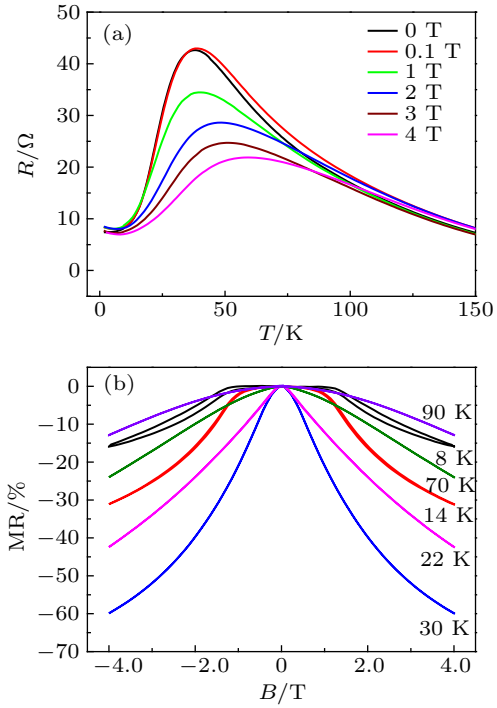


Fig. 4. (a) The temperature dependence of resistivity of 10-nm EuS/Nb:STO junction measured in various magnetic field, the sharp decrease of R indicates the onset of ferromagnetic transition; (b) magnetoresistance of the EuS/Nb:STO junction as a function of magnetic field at various temperature; the hysteretic behavior displayed at $T = 8$ K.

To get further insight into the negative MR effect in this heterojunction, the MR as a function of magnetic field for various temperature is shown in Fig. 4(b), the MR calculations has been defined as

$$\mathrm{MR} = [R(B) - R(0)]/R(0) \times 100\%,$$

where $R(B)$ and $R(0)$ are the resistance in presence and in absence of external magnetic field respectively. The MR effect is not related with spin–orbit interaction arising from Pt electrode.[30] Similar to the MR results obtained at 4.2 K in bulk EuS material,[28] a butterfly shape of negative hysteretic MR is observed at 8 K. At 8 K, the magnetizations are not saturated for sufficiently high field (~ 4 T), the hysteretic behavior disappears at 30 K. In low-field magnetoresistance, the hysteretic effect arises from various anisotropies (magnetocrystalline anisotropy, anisotropic magnetoresistance, and colossal magnetoresistance).[31] The high-field hysteretic effect is also observed in EuS film grown on GaAs, but the origin of it is still unclear. The hysteresis of Hall effect of EuS bulk reported by Shapira *et al.*[28] was observed in Eu-rich samples at $H < 8.5$ T and was proportional to H ($H > 8.5$ T), indicating the hysteresis relates to the changes in Hall carrier concentration. Below about 30 K this MR steadily increases with increasing temperature, and is consistent with the spin-filtering behavior. However, the stoichiometric EuS thin film exhibits insulating property at low temperature, thus it unable to measure the resistance due to equipment limit, it is difficult to estimate the contribution of the intrinsic MR of EuS film. The negative MR at 30 K experiences a 60% improvement at 4 T, comparing the one without applied field. As seen in Fig. 4(b), the MR effect still exists even the temperature is up to 90 K, which enables the application of this junction over a wide temperature range. The tunneling effect above T_c can be described by a critical scattering model,[32] the short range magnetic fluctuations is dominate in a paramagnetic environment, the exchange interaction between a free carrier and local spin can cause electron localization into an ferromagnetic droplet[33] on the scale of the lattice spacing in the paramagnetic region. The charge carrier is accompanied by reorientations of local spins to from its immediate ferromagnetic environment, during the electron in the barrier region can be scattering by magnetic fluctuations which leads to a remarkable reduction of the carrier mobility, and thus the resistance is proportional to the amount of this scattering.

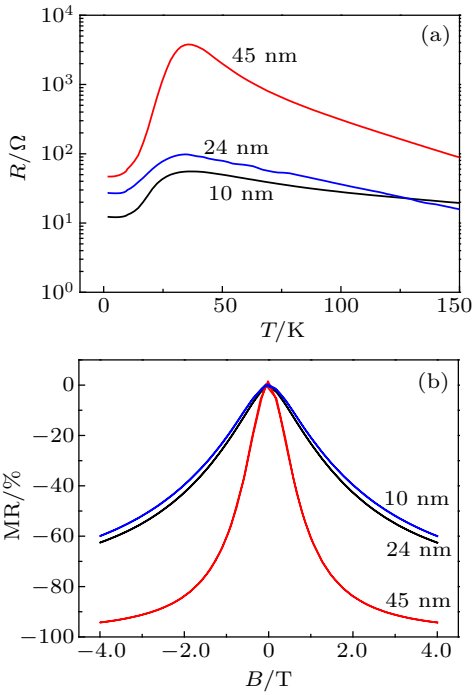


Fig. 5. (a) R–T curve and (b) magnetoresistance (at 30 K) of the junction with EuS barrier of 10 nm, 24 nm, and 45 nm.

It is well known the barrier height at fixed temperature is constant. However, the spin filtering of EuS is relevant to exchange splitting to filter spins, thus, a larger exchange splitting of the condition band should be expected in thicker EuS barrier.[14] The R_J increases with increasing EuS barrier thickness. It indicates the origins of charge carriers is mostly from EuS/Nb:STO interface. With the EuS layer up to 45 nm, the R_J is up to 3.7 kΩ at zero-field, as shown in Fig. 5(a). It is

also observed the transition temperature slightly improved for the sample with the thicker EuS barrier. This is the general behavior of ferromagnetic films, observed by Santos *et al.*[14] and Muller *et al.*[34] This trend is caused by the lower coordination of the Eu^{2+} ions at the interfaces, such that the increasing atomic surface-to-volume ration for the thinner films leads to weaker exchange interactions. The data for MR ratio depends on EuS barrier thickness shown in Fig. 5(b), the MR ratio increases monotonically as EuS barrier increases. The junction conductance is reduced with EuS barrier thickness increasing, the tunneling process could be simplified into a qualitative model of a free-electron incident on a square barrier of height and thickness d,[35,36] thus a large magnetoresistance that increases with barrier thickness is predicted. The MR ratio reaches to 95% at 30 K with 45-nm EuS barrier, meanwhile, the resistance drops abruptly in low-field range from 0 T to 1 T.

4. Conclusions

In conclusion, we observed that the single crystal EuS films grown on Nb:STO leads to good magnetic and transport properties of the barrier layer. A paramagnetism-to-ferromagnetism temperature is improved as high as 35 K due to additional charge carriers doping in the interface of junction. In this junction, a large magnetoresistance is observed in a wide temperature region. The large negative MR may be attributed to the spin-filter characteristics of the interfacial EuS layer below T_c and electron scattering by magnetic fluctuations above T_c. The MR ratio is 60% at 30 K, and even 13% at 90 K in EuS (10 nm)/Nb:STO. The MR ratio could be enhanced to 95% with EuS layer thickness increases to 45 nm. Thus, the EuS/Nb:STO semiconductor junction is powerful for considering as a high efficiency spin injector and spin detector in spintronic devices.

References

[1] Prinz G A 1998 *Science* **282** 1660
[2] Gupta A and Sun J Z 1999 *J. Magn. Magn. Mater.* **200** 24
[3] Jr. R J S, Byers J M, Osofsky M S, Nadgorny B, Ambrose T, Cheng S F, Broussard P R, Tanaka C T, Nowak J, Moodera J S, Barry A and Coey J M D 1998 *Science* **282** 85
[4] Moodera J S, Santos T S and Nagahama T 2007 *J. Phys.: Condens. Matter* **19** 165202
[5] Nagahama T, Santos T S and Moodera J S 2007 *Phys Rev Lett.* **99** 016602
[6] Senapati K, Blamire M G and Barber Z H 2011 *Nat. Mater.* **10** 849
[7] McGuire T R, Argyle B E, Shafer M W and Smart J S 1962 *Appl. Phys. Lett.* **1** 17
[8] VanHouten S 1962 *Phys. Lett.* **2** 215
[9] Wachter P 1979 *Handbook on the Physics and Chemistry of Rare Earths* (Elsevier) pp. 507–574
[10] A. Mauger and Godart C 1986 *Phys. Rep.* **141** 51
[11] Zinn W 1976 *J. Magn. Magn. Mater.* **3** 23
[12] Esaki L, Stiles P J and Molnar S v 1967 *Phys. Rev. Lett.* **19** 852
[13] Moodera J S, Hao X, Gibson G A and Meservey R 1988 *Phys. Rev. Lett.* **61** 637
[14] Santos T S, Moodera J S, Raman K V, Negusse E, Holroyd J, Dvorak J, Liberati M, Idzerda Y U and Arenholz E 2008 *Phys. Rev. Lett.* **101** 147201
[15] Muller M, Schreiber R and Schneider C M 2011 *IEEE Trans. Magn.* **47** 1635
[16] Caspers C, Müller M, Gray A X, Kaiser A M, Gloskovskii A, Fadley C S, Drube W and Schneider C M 2011 *Phys. Rev. B* **84** 205217
[17] Panguluri R P, Santos T S, Negusse E, Dvorak J, Idzerda Y, Moodera J S and Nadgorny B 2008 *Phys. Rev. B* **78** 125307
[18] Fumagalli P, Schirmeisen A and Gambino R J 1998 *Phys. Rev. B* **57** 57
[19] Ren C, Trbovic J, Xiong P and von Molnár S 2005 *Appl. Phys. Lett.* **86** 012501
[20] Guilaran I J, Read D E, Kallaher R L, Xiong P, von Molnár S, Stampe P A, Kennedy R J and Keller J 2003 *Phys. Rev. B* **68** 144424
[21] Hao X, Moodera J S and Meservey R 1990 *Phys. Rev. B* **42** 8235
[22] O'Mahony D, Smith C, Budtz-Jorgensen C, Venkatesan M, Lunney J G, McGilp J F and Coey J M D 2005 *Thin Solid Films* **488** 200
[23] Yang Q I, Zhao J, Zhang L, Dolev M, Fried A D, Marshall A F, Risbud S H and Kapitulnik A 2014 *Appl. Phys. Lett.* **104** 082402
[24] Stachow-Wójcik A, Story T, Dobrowolski W, Arciszewska M, Gałązka R R, Kreijveld M W, Swüste C H W, Swagten H J M, de Jonge W J M, Twardowski A and Sipatov A Y 1999 *Phys. Rev. B* **60** 15220
[25] Demokritov S, Rticker U and Grtinberg P 1996 *J. Magn. Magn. Mater.* **163** 21
[26] Li X L and Xu X H 2019 *Chin. Phys. B* **28** 098506
[27] Ziese M, Köhler U, Bollero A, Höhne R and Esquinazi P 2005 *Phys. Rev. B* **71** 180406
[28] Shapira Y and Reed T B 1972 *Phys. Rev. B* **5** 4877
[29] De Gennes P G and Friedel J 1958 *J. Phys. Chem. Solids* **4** 71
[30] Lomicronpez-Mir L, Frontera C, Aramberri H, Bouzehouane K, Cisneros-Fernandez J, Bozzo B, Balcells L and Martinez B 2018 *Sci. Rep.* **8** 861
[31] O'Donnell J, Onellion M, Rzchowski M S, Eckstein J N and Bozovic I 1997 *Phys. Rev. B* **55** 5873
[32] Thompson W A, Holtzberg F, McGuire T R and Petrich G 1972 *Magn. Magn. Mater. AIP Conf. Proc.* **5** 827
[33] Zhu L Q, Lin T, Guo S L, and Chu J H 2012 *Acta Phys. Sin* **61** 087501 (in Chinese)
[34] Müller M, Schreiber R and Schneider C M 2011 *J. Appl. Phys.* **109** 07C710
[35] Pan L F, Wen H Y, Huang L, Chen L, Deng H X, Xia J B and Wei Z M 2019 *Chin. Phys. B* **28** 107504
[36] Butler W H, Zhang X G, Schulthess T C and MacLaren J M 2001 *Phys. Rev. B* **63** 054416